

© 2015

LAURA NATALIA GONZALEZ BUSTACARA

ALL RIGHTS RESERVED

STUDY OF THE EFFECT OF THE ENVIRONMENTAL RELATIVE HUMIDITY ON THE  
ANGLE DEPENDENT PEELING STRENGTH OF PRESSURE SENSITIVE ADHESIVES  
(PSA)

A Thesis  
Presented to  
The Graduate Faculty of The University of Akron

In Partial Fulfillment  
of the Requirements for the Degree  
Master of Science

Laura Natalia Gonzalez Bustacara  
August, 2015

STUDY OF THE EFFECT OF THE ENVIRONMENTAL RELATIVE HUMIDITY ON THE  
ANGLE DEPENDENT PEELING STRENGTH OF PRESSURE SENSITIVE ADHESIVES  
(PSA)

Laura Natalia Gonzalez Bustacara

Thesis

Approved:

Accepted:

---

Advisor  
Dr. Ali Dhinojwala

---

Dean of the College  
Dr. Eric J. Amis

---

Faculty Reader  
Dr. Abraham Joy

---

Dean of the Graduate School  
Dr. Chand Midha

---

Department Chair  
Dr. Coleen Pugh

---

Date

## ABSTRACT

The use of adhesives, especially pressure sensitive adhesives (PSA), has relevance in many industrial, medical and commercial applications such as automotive, aerospace, biomedical and electronics.

A number of characterization techniques have been used with the main purpose of understanding the performance of PSA by quantifying material properties, such as peeling strength. The peeling strength is dependent on the composition, viscoelastic properties of the adhesive, and its measurement provides information regarding stickiness and reversibility on different substrates [1-3].

The work of Kendall and Gent [3, 4] explained the dependence of peeling force on peeling angle, work of adhesion and the modulus of the adhesive tape. Although the measurement of peeling strength has been widely studied, few experiments have explored the effect of humidity and temperature on peel strength.

In this work we have used the Kendall approach to evaluate the effect of humidity on the peel strength of PSA at constant temperature (23°C). Our results

confirm the expected angle dependence of the peel strength, being considerably superior when small angles were tested.

Furthermore, our results indicate that the peel strength is reduced with increased humidity. Understanding the influence of humidity on adhesion will help provide insight to the humidity response of biological adhesives used by spiders and geckos [5, 6].

## ACKNOWLEDGEMENTS

I express my sincere gratitude to my research advisor professor Ali Dhinojwala for his continuous encouragement, guidance and practical lessons on science and engineering since I joined his research group. I also thank Dr. Abraham Joy for agreeing to serve as my committee member. I extend my gratitude to Dr. Gary Hamed for his support during several critical and interesting discussions, providing me crucial and inspiring information that helped me a lot during the research and experimental phase of this study. Thanks to Mr. Edward Laughlin for their support on machining and modification of my apparatuses.

I also thank my colleagues of the department of Polymer Science for their friendship and support. Thanks to my closest friends for making my life in and outside of the school more enjoyable. I express very special gratitude to Zachary Zander for his assistance, time and support from the beginning to the end of the years that we studied together.

Last but certainly not least, I dedicate this work to my parents Germán Alirio González and Paulina Bustacara, my brother Germán Leonardo and my sister Paula Valentina who have supported every step of my life and for making it possible that I am able to achieve my goals.

## TABLE OF CONTENTS

	Page
LIST OF FIGURES .....	viii
LIST OF TABLES .....	x
CHAPTER	
I INTRODUCTION .....	1
II BACKGROUND.....	3
2.1. Energy theory of fracture for an elastic film - Kendall's Model.....	3
2.2. Peeling Test.....	7
2.3. Experimental Apparatus Currently Used for Peeling Test.....	9
2.4. State of the Art of Peeling Force Measurements.....	11
2.5. State of the Art of the Effect of Humidity on Adhesive Systems.....	12
2.6. Statement of Purpose.....	13
III EXPERIMENTAL.....	15
3.1. Sample Preparation.....	15
3.2. Peeling Test.....	17
3.3. Experimental Setup.....	20
3.4. Testing Conditions .....	23

IV RESULTS AND DISCUSSION .....	25
4.1. Material Selection.....	25
4.2. Variation of Peel Strength with Crack Speed and Humidity Effect on Peeling Rate. ....	28
4.3. Single Layer vs. Multi-layer Adhesive Systems.....	32
4.4. Effect of Humidity on the Peeling Strength Dependent on the Peeling Angle.....	35
V SUMMARY AND CONCLUSIONS.....	43
REFERENCES .....	45
APPENDICES.....	48
APPENDIX A: PEELING STRENGTH DEPENDENT ON THE PEELING ANGLE. DATA COLLECTED AT LOW RELATIVE HUMIDITY ( $\leq 35\%$ ).....	49
APPENDIX B: PEELING STRENGTH DEPENDENT ON THE PEELING ANGLE. DATA COLLECTED AT MEDIUM RELATIVE HUMIDITY ( $\cong 55\%$ ) .....	50
APPENDIX C: PEELING STRENGTH DEPENDENT ON THE PEELING ANGLE. DATA COLLECTED AT HIGH RELATIVE HUMIDITY ( $\geq 75\%$ ).....	51



## LIST OF FIGURES

Figure	Page
2.2. Schematic of the peeling-off system. Thin film adhered to glass substrate.....	3
2. 3. Variation of 90° peel strength with crack speed $c$ .....	6
2.4. Peel strength dependence on peel angle. Constant crack speed of 80 $\mu\text{m/s}$ . (Determined from Figure 2.2.).....	7
2.5. Common industrial methods currently used for evaluating the peel off force: (a) 90° peel off test, (b) 180° peel off test, and (c) t-peel test. ....	9
2.6. (A) Peeling test at 90° using a universal testing machine. (B) Peeling test using a universal testing machine with mobile platform to adjust the peeling angle .....	10
3.1. Final sample configuration possessing two strips ( $b=1\text{ cm}$ ) of Magic Scotch Tape 3M® (2 samples per glass slide).....	17
3.2. Animation of the peeling test setup including the modification to achieve small peeling angles. ....	18
3.3. Peeling test geometry. (A) Peeling off from the lower edge. (B) Peeling off from the superior edge. ....	19
3.4. Complementary experimental tools. (A) Set of calibrated weights. (B) Timer and basket as a load holder.....	21
3.5. The measuring ruler on the base of the sample holder; testing area is marked in pink ranging from 2-5 cm over the sample test.....	22
3.6. The traceable hygrometer (A) allows for precise adjustments of the temperature and RH, the dehumidifier (B) lowers the RH, and the humidifiers (C) increase the RH as needed. ....	24

4.1. Optical Microscopy with 2X magnification, showing the contact homogeneity of (A) Masking Tape 3M® in contact with glass substrate and (B) Magic Scotch Tape 3M® in contact with glass substrate. Scale bar= 200 $\mu\text{m}$ . .....	27
4.2. Schematic representation of a single coated pressure sensitive adhesive .....	33
4.3. Relationship between the peel force and the peel angle.....	34
4.4. Rivlin Model for the peel strength dependence on peel angle at low (green), medium (red) and high (blue) relative humidity. Measurements taken at crack speed range between 200 $\mu\text{m/s}$ to 300 $\mu\text{m/s}$ . ....	36
4.5. Kendall Model for the peel strength dependence on peel angle at low (green), medium (red) and high (blue) relative humidity. Measurements were taken at a crack speed range between 200 $\mu\text{m/s}$ to 300 $\mu\text{m/s}$ . ....	36

## LIST OF TABLES

Table	Page
4. 2. Speed Measurement Data at $\pi/2$ ( $90^\circ$ ) .....	29
4. 3. Results obtained from the fitting curves and calculated elastic modulus ....	38

## CHAPTER I

### INTRODUCTION

The use of adhesives to bond separated parts and materials together dates from ancient times when the Greeks and Romans adopted natural materials (such as blood, milk, egg whites, etc.) to develop adhesives. Nevertheless, it was only in the 19th Century when pressure sensitive tape was invented by the surgeon, Horace Day, who coated strips of fabric with a rubber adhesive in a successful attempt to make the first surgical tape [7].

Nowadays, pressure sensitive adhesives, have a broad use in large number of industrial, medical and commercial applications. The versatility of these materials have allowed them to flourish in a range of markets, including the automotive and aerospace industry, tissue engineering, precision instruments, as well as in daily life. Consequently, the accurate characterization of the performance of adhesives represents a crucial and sometimes challenging research area.

A wide number of characterization techniques have been used with the main purpose of understanding the performance of these pressure sensitive

adhesives. These techniques help quantify material properties such as tensile and shear strength, elastic moduli and fracture mechanics, as well as peeling strength. The peel strength is dependent on the composition and the rheological properties of the adhesive, and its measurement produces information pertaining to the stickiness and removability to and from different substrates [1-2, 7].

In this work, the effects of the peeling angle on the peeling strength of an adhesive thin film to a glass substrate were studied as a review of the analysis proposed by Dr. K Kendall in 1975.

Furthermore, a new approach is evaluated in this study with the inclusion of an additional experimental variable, the environmental relative humidity (RH), and its effect on the angle dependent adhesion strength of pressure sensitive acrylate-based adhesives is analyzed.

The overall goal of this project is to establish an adaptation and optimization of a reproducible experimental model proposed by Dr. Kendall, to be implemented in the characterization of humidity responsive biological adhesives.

## CHAPTER II

### BACKGROUND

#### 2.1. Energy theory of fracture for an elastic film - Kendall's Model [4].

In 1975, Dr. Kendall published an article called "Thin-film peeling – the elastic term," which presented a model describing the influence of different variables on the peeling strength using an energy balance for a system that includes a thin elastic film and a rigid substrate. The system used for these experiments is presented in Figure 2.1. The thickness of the thin film is represented as  $d$ , the width is  $b$ , the displacement is  $\Delta c$ , and the elastic modulus is  $E$ . The peeling angle is shown as  $\theta$  and the loaded force is  $F$ .

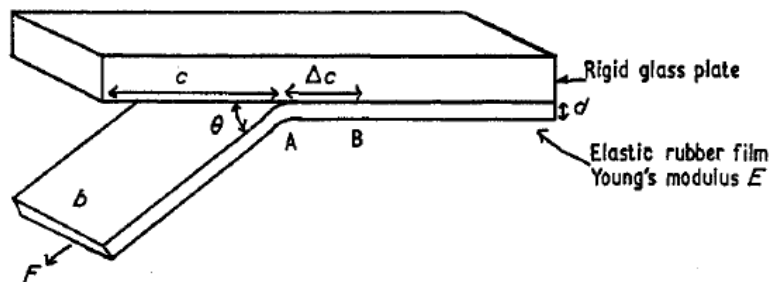


Figure 2.1. Schematic of the peeling-off system. Thin film adhered to glass substrate [4]

In the conservation of energy expression, there are contributions from three different terms. The surface energy term, shown in equation (1), describes the energy required to create new surfaces. From this term, it is possible to define adhesive energy (R) as a new variable, corresponding to the energy required to create new surfaces per unit area. In addition, R is peeling rate dependent, b is the sample width, and  $\Delta c$  is the displacement.

In the conservation of energy expression, there are contributions from three different terms. The surface energy term, shown in equation (1), describes the energy required to create new surfaces. From this term, it is possible to define adhesive energy (R) as a new variable, corresponding to the energy required to create new surfaces per unit area. In addition, R is peeling rate dependent, b is the sample width, and  $\Delta c$  is the displacement.

$$bR\Delta c \quad (1)$$

The second energetic contribution corresponds to potential energy. This energy is the work done, accounting for the effect of the motion of the loaded force, and ignoring the extensibility of the film. This assumption allows for the relationship between the force (F), the displacement ( $\Delta c$ ) and the angle ( $\Theta$ ), as shown in equation (2).

$$F(1 - \cos\Theta)\Delta c \quad (2)$$

Despite the previous assumption, it's appropriate to consider the elasticity of the film independently. Stretching in region AB (Figure 2.1) of the sample is expected since the experiment involves hanging a weight in order to generate movement that can be described using the Hooks Law, since it moves as a spring. For this reason, it is necessary to include an elastic term in the energy balance. The elastic term has two contributions: a contribution correspondent to the stretching of the region AB (3.1) and a contribution from the energy stored in the stretched material (3.2). E corresponds to the elastic modulus of the material and d is the film thickness.

$$\frac{F^2 \Delta c}{bdE} \quad (3.1)$$

$$- \frac{F^2 \Delta c}{2bdE} \quad (3.2)$$

After adding the individual energies and upon further simplification, the general energy balance can be presented as follows:

$$\left(\frac{F}{b}\right)^2 \frac{1}{2dE} + \left(\frac{F}{b}\right) (1 - \cos\theta) - R = 0 \quad (4)$$

Equation 4 is a quadratic equation with the ratio of the peeling force (F) and the width of sample (b) as a new variable (F/b), which is defined as peeling strength.

In order to be able to apply Equation (4), it is appropriate to measure the force F at an angle of  $\theta = \pi/2$ . The contribution of the elastic term



corresponding to an angle of  $90^\circ$  tends to zero and can be neglected, allowing for the expression of adhesive energy ( $R$ ) as a function of the experimental crack speed ( $\dot{c}$ ), shown in equation (5).

$$\left(\frac{F}{b}\right) = R(\dot{c}) \quad (5)$$

Once the values of crack speed have been measured, it is possible to plot the variation of  $90^\circ$  peel strength with crack speed  $\dot{c}$  as seen in Figure 2.2.

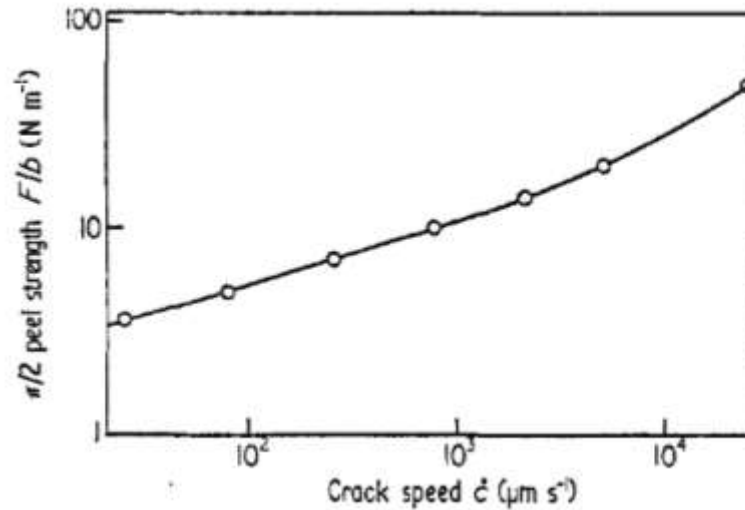


Figure 2. 2. Variation of  $90^\circ$  peel strength with crack speed  $\dot{c}$  [4]

From this plot, the adhesive energy can be determined by only two variables: angle and peel strength, which can be utilized to construct a plot showing the dependence of peel strength on peel angle at a constant crack speed. Figure 2.3 shows the data obtained for ethylene propylene rubber

adhered to glass a glass plate, as well as the theoretical predictions when no extension and pure extension is considered. [4]

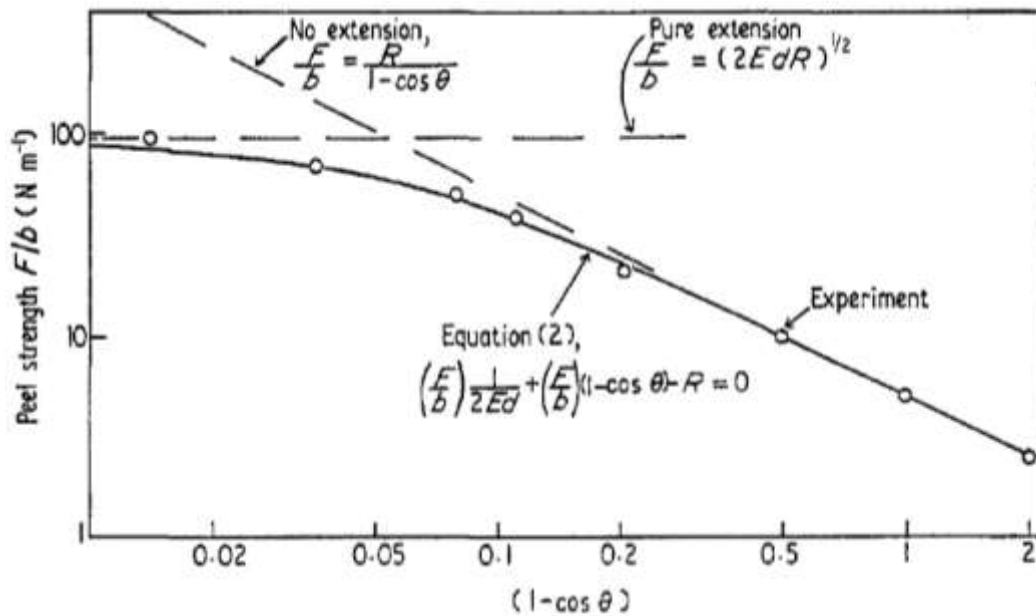


Figure 2.3. Peel strength dependence on peel angle. Constant crack speed of 80  $\mu\text{m/s}$ . (Determined from Figure 2.2.)

## 2.2. Peeling Test

The peeling test is one of the most important measurements used to characterize adhesives. This experiment is performed with the objective of determining the forces at the interface between particles and surfaces, such as the adhesion energies of solid surfaces in contact and particle adhesion forces.

The results have general applications in adhesive tapes, crack propagation, and material fracture [8].

Experiments on peeling that measure the peeling strength can provide information about the rheological properties of a specific material, as well as its removability.

These experiments have been mentioned since the 1950s, when the force required to peel a metal glued to a rigid glass plate with a polymeric adhesive was determined [9]. In 1975, Kendall proposed an energy balance, highlighting the existence of an elastic term as a determinant aspect of the thin film peeling off from a rigid substrate. This energy balance was based on the measurements of the peeling force and its dependence on the peeling rate and peeling angle.

Peeling force measurements are highly affected by the geometry and configuration of the test. Primarily, three peeling test configurations are used, including  $\Theta=180^\circ$ ,  $\Theta=90^\circ$ , and the T-peeling test. Nowadays, the tests are performed following ASTM standards, such as the procedure described in “ASTM D 3330/D 3330M Test Method for Peel Adhesion of Pressure-Sensitive Tape,” which specifies the conditions to evaluate peeling force in three different methods, as shown in Figure 2.4 [10].

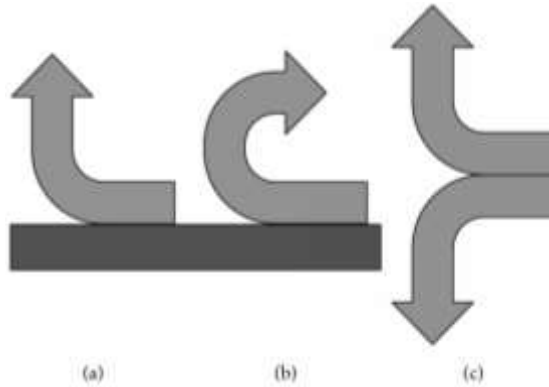


Figure 2.4. Common industrial methods currently used for evaluating the peel off force: (a) 90° peel off test, (b) 180° peel off test, and (c) t-peel test.

### 2.3. Experimental Apparatus Currently Used for Peeling Test

Different types of instruments can be used to obtain peeling strength data from the three testing configurations. The Universal Testing Machine, also used for tensile strength measurements, is one of the most commonly used. The advantage of using this equipment is that it allows for control of the applied force needed to remove the tape from the substrate, as shown in Figure 2.5. (A).

These experiments yield interesting and valuable results for a wide range of adhesive systems; however, it is not realistic to assume that all systems can be accurately described using these three configurations, especially in the field of biomechanics where complex biological systems like spider silk attachment or gecko toe dry adhesives are examined.

According to Kovalchic et al. [11], the implementation of a mobile platform as a sample holder to the previously described system, depicted in Figure 2.5. (B), permits the adjustment of the desired peeling angle. Nevertheless, the data collected from these experiments are only provided for angles higher than  $30^\circ$ , and previous works (Kendall, 1975) have demonstrated a higher impact in the adhesion performance when the peeling is done at small angles ( $\leq 30^\circ$ ). Thus, peeling test at different angles (especially at small angles) is still experimentally challenging to perform.

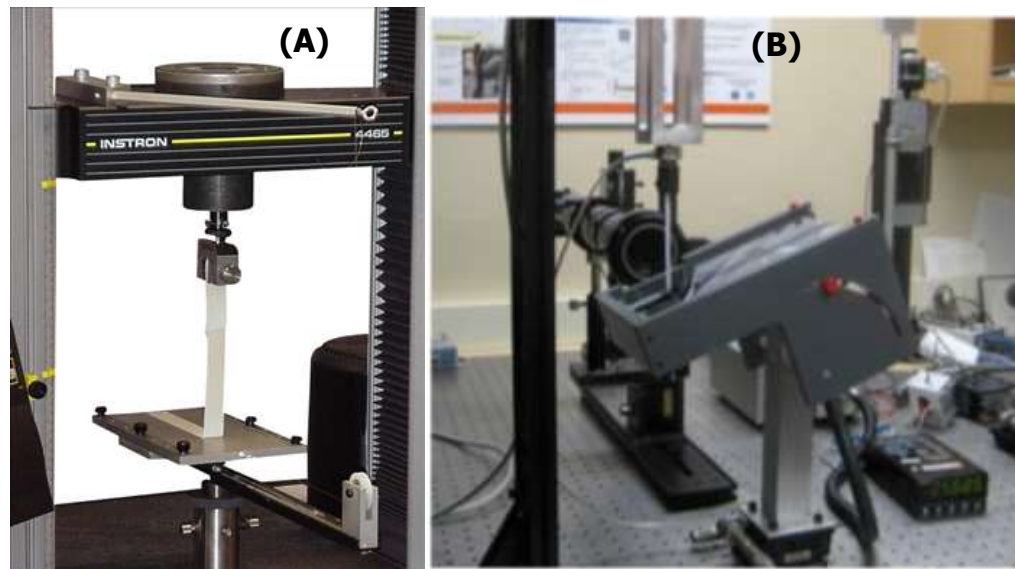


Figure 2.5. (A) Peeling test at  $90^\circ$  using a universal testing machine [18]. (B) Peeling test using a universal testing machine with mobile platform to adjust the peeling angle [11].

## 2.4. State of the Art of Peeling Force Measurements

Most of the developments in this field have occurred in response to empirical observations that have demonstrated the need for considering the adhesion force as a vital part of our current understanding of the adhesion phenomena, particularly in biological systems.

The analysis of all of these systems can be benefited by the appropriate characterization of the adhesion forces and their dependence on the angle and the effect of the varying environmental conditions, such as temperature and humidity.

Another interesting article, published in 2007 by Pesika et al. [12], presented a model based on the description (and subsequent addition to the Kendall model) of the peel zone (PZ). This was developed to show the behavior of adhesive tapes and their dependence on the peel angle, specifically at  $90^\circ$  or less. Experimental measurements were performed on three different tapes with varying physical properties, i.e. adhesive strength, bending moduli and stretch moduli. The results were compared with the model, concluding that a peel angle of  $18.4^\circ$  is the characteristic peeling angle in which the highest adhesion strength is exhibited for a gecko adhesive system.

The conclusions of the aforementioned article were utilized in the study of Gecko inspired biomimetic bidirectional switchable adhesive, published by Jin, K. et al in 2014 [13], in which the authors found that the adhesion forces are

enhanced due to the influence of small angles at the moment of peeling off the fibers from a substrate.

In terms of the experimental design, Roenbeck et al. [14] proposed an alternative method to perform peeling tests on the nano-scale, and implemented a finite element analysis to confirm the applicability of Kendall's Model.

Most recently, an article published by Brely et al. [15] introduced the Multiple Peeling Theory (MPT), in which they show that "a multiple peeling problem can be treated as the superposition of single peeling configurations even for complex structures".

## 2.5. State of the Art of the Effect of Humidity on Adhesive Systems

The effect of moisture on pressure sensitive adhesion has been previously studied, focusing on the changes on the material properties.

The effect of humidity on PSA films was studied by Houtman et al. [16] The authors mentioned that the stabilization of hydrophobic polymer particles after emulsion polymerization is achievable using done by the use of surfactants. The authors claim that these surfactants generate "pathways" that allow the water to penetrate the film. Films with high content of surfactants demonstrate considerable differences in the mechanical properties for dry and wet samples. Tensile strength experiments were performed and the results from dry and wet

samples were compared, showing a decrease in the adhesion strength as a result of the humidity applied.

The humidity response of biological adhesives has also been studied, mainly for geckos and spiders.

Niewiarowski et al. [5] tested the dependence of the adhesion properties on the temperature and relative humidity for two different species of geckos. Their findings have important conclusions such as the improvement of the adhesion ability when the tests were performed at low temperature and high humidity environmental conditions, that helped develop the understanding of the clinging mechanisms and humidity effects in gecko toe pad adhesion.

Studies on spider silk developed by Agnarsson et al. [6], demonstrated how the cyclic super-contractions exhibited by spider silk when subjected to changes in humidity are similar to the contractions present in human muscles. The findings from this research can lead to potential applications of spider silk as a biomimetic muscle with unique properties for humidity response sensors or actuators.

## 2.6. Statement of Purpose

Although the measurement of peeling strength have been widely studied because of its importance to understanding adhesive behavior, only a few ideas



have been explored related to this property under diverse environmental conditions. A novel approach is presented in this study to evaluate the effect of peeling angle and environmental humidity variation in the peeling strength exhibited by pressure sensitive adhesives. These studies are of great importance at the industrial level; especially in fields involving biomechanics such as spider silk adhesives and gecko dry adhesives, as these findings are fundamental to explain the adhesive mechanisms of new materials. As a base line, the work performed by Dr. Kendall has been taken, since this was the first concrete and concise approximation of the effect of peeling angle variation on peeling systems of thin film, polymer-based materials.

## CHAPTER III

### EXPERIMENTAL

#### 3.1. Sample Preparation

Thoroughly cleaned laboratory glass slides were used as the substrate. The cleaning procedure involved initially rinsing the new slides with acetone, followed by distilled water. The slides were not used a second time because the results were affected by scratches and residual impurities in the glass, due to cohesive failure of the adhesive.

The glass slides were placed in a base bath containing KOH and isopropyl alcohol dissolved in water for duration of 1 to 2 hours. Subsequently, each glass slide was fully rinsed with copious amounts of distilled water. Finally, slides were dried using nitrogen and stored in a dry and clean place until use.

At some point, Octadecyltrichlorosilane (OTS) coating treatment was considered, however, the results did not represent significant difference when compared to the non-treated slides, and thus OTS coating treatment was discarded.

With regard to the selected material, thin strips of approximately 1 cm of Polyisoprene NATSYN 2200 from Goodyear Chemical, made by compression

molding, were suggested as testing material to fully reproduce Kendall's experiments that yielded the analysis described in section 2.1 of this document and used previously in associated research [17].

However, after using this material in several trials without consistent results, it was decided to switch to Masking Tape 3M<sup>®</sup> because it was assumed to be a more controllable system. In this case, the width of the tape was  $\frac{3}{4}$ ". Initially, the experiments were performed at room temperature and relative humidity conditions.

The results yielded by Masking Tape 3M<sup>®</sup> were not consistent and will be presented in Chapter IV corresponding to Results and Discussion.

A new material, Magic Scotch Tape 3M<sup>®</sup> was chosen after noticing that it has been used in multiple peeling test papers performed by previous research groups, with consistent results [11].

Once the glass slides were cleaned and dried the samples were made by placing a piece of tape carefully taken from the roll and pressing uniformly against the substrate; making sure that full contact between adhesive and substrate was achieved. A piece of rubber was used to apply the pressure evenly over the surface. From Section 2.1, we know that the peeling strength is dependent on the width of the film. The total width of the tape ( $\frac{3}{4}$ "") was divided in three sections using a razor blade, and the middle portion was removed in order to avoid attachments between the three tape parts that could affect the

performance of the experiment. The width ( $b$ ) of each sample is then  $\frac{1}{4}$ ". Figure 3.1. shows the final configuration of the sample with the reinforcement on one of the edges for the weight to be hung.



Figure 3.1. Final sample configuration possessing two strips ( $b=1$  cm) of Magic Scotch Tape 3M<sup>®</sup> (2 samples per glass slide).

### 3.2. Peeling Test

A schematic overview of the testing setup is illustrated in Figure 3.2. The peeling test was performed using a device similar to the one used by Dr. Kendall in his work.



Figure 3.2. Animation of the peeling test setup including the modification to achieve small peeling angles.

The wooden structure is meant to be an inclined plane that has a slide holder to place the system substrate - sample to be tested. Its slope angle can be adjusted to the angle required using a metallic protractor, considering that the peeling angle  $\Theta$  is a function of the  $\Theta_{\text{Observed}}$  that is displayed by the instrument. Equation (6-1) shows the calculation of  $\Theta$  when the sample is peeled from the inferior edge (Figure 3.3. (A)). For instance, if the desired angle is  $60^\circ$ , the angle chosen from the metallic protractor should be  $30^\circ$  and the peeling should be done from the lower edge of the tape.

$$\Theta = (90 - \Theta_{\text{Observed}}) \quad (6-1)$$

On the other hand, when the tape is peeled from the superior edge (Figure 3.3. (B)), the value of  $\Theta$  is determined by Equation (6-2). This means that if the desired angle is  $120^\circ$ , then the angle marked on the metallic protractor should be  $30^\circ$ , but in this case the peeling should be done from the superior edge of the tape.

$$\Theta = (90 + \Theta_{\text{Observed}}) \quad (6-2)$$

Some modifications were made to the original design, for instance, the inclusion of a metallic vertical bar with the purpose of achieving small angles ( $5^\circ$  to  $30^\circ$ ), as shown in figure 3.2.

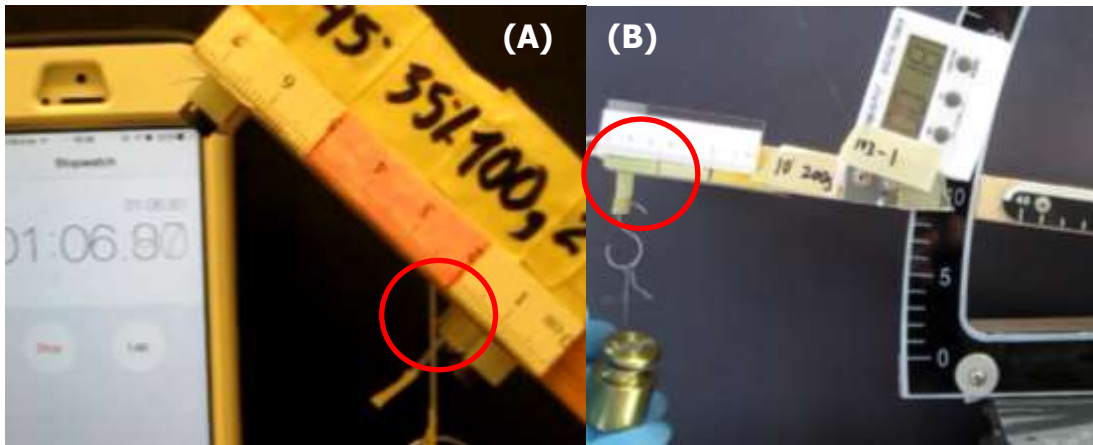


Figure 3.3. Peeling test geometry. (A) Peeling off from the lower edge. (B) Peeling off from the superior edge.

### 3.3. Experimental Setup

The prepared sample (Figure 3.1.) was fixed in the designated place beneath the inclined plane and secured with screws. This region also has a ruler that allows for measurements of the tape displacement.

The system was then labeled to avoid another tilting besides the one setup in the plane.

The measurements were made by applying a pendant load on the system. A set of calibrated weights (Figure 3.4. (A)) were hung with a hook from the reinforced edge of the sample using a plastic basket as a weight holder (Figure 3.4. (B)). Once the load was applied, gravitational forces caused the adhesive sample to begin peeling off. The displacement was registered by video (one of the videos is presented in the supporting information), using a small ruler located over the glass slide holder (Figure 3.4. (B)), to mark the different positions of the sample along the glass substrate with time. A stopwatch was used to measure the time required for the sample to move from the initial to the final position. This information was needed to determine the peeling rate.

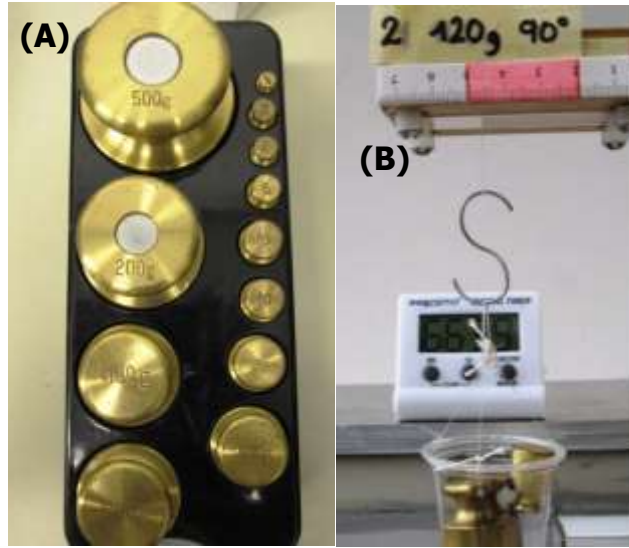


Figure 3.4. Complementary experimental tools. (A) Set of calibrated weights. (B) Timer and basket as a load holder

The experiments were divided in Part 1 and Part 2 following the procedures from Kendall's work.

Part 1 was intended to determine the variation of the peel strength with crack speed ( $\dot{c}$ ) at a constant angle. Therefore, the fixed parameter is the angle ( $90^\circ$ ) and under this condition the elastic component of the energy balance presented in equation 4 can be neglected. Removal of the elastic component allows for the variation of  $90^\circ$  peel strength with crack speed ( $\dot{c}$ ) profile to be constructed, as shown in Figure 2.2.

In part 1, a total of three samples were tested at seven different loads: 30g, 40g, 50g, 60g, 70g, 80g, 100g; for each of the three environmental configurations: low ( $\leq 35\%$  Relative Humidity), medium ( $\cong 55\%$  Relative



Humidity) and high ( $\geq 75\%$  Relative Humidity). The edges of the sample were neglected because a constant pressure and a uniform contact can be only ensured on the middle region (from 2 cm to 5 cm) in the sample. Individual samples were additionally divided into three segments of one centimeter each defining three regions from 2cm to 3cm, 3cm to 4cm and 4cm to 5cm (or vice versa) over the measuring ruler as it can be seen in Figure 3.5.

In this manner, 63 data points were collected for each of the three humidity conditions, resulting in 189 data points collected for part 1 of the experiment. With this data the rate was calculate and the constant crack speed ( $\dot{c}$ ) was determined, which is the fixed parameter in part 2 of this study.



Figure 3.5. The measuring ruler on the base of the sample holder; testing area is marked in pink ranging from 2-5 cm over the sample test.

Part 2 aims to determine the effect of humidity on peeling strength at different peeling angles.

Once again, three samples were tested for the selected crack speed  $\dot{c}$ , in this case between 200 and 300  $\mu\text{m}/\text{sec}$ , and specific loads were estimated for eight different angles:  $15^\circ$ ,  $30^\circ$ ,  $45^\circ$ ,  $60^\circ$ ,  $90^\circ$ ,  $105^\circ$ ,  $120^\circ$ ,  $135^\circ$ ; for each of the three environmental configurations: low ( $\leq 35\%$  Relative Humidity), medium ( $\cong 55\%$  Relative Humidity) and high ( $\geq 75\%$  Relative Humidity). The edges of the sample were neglected because a constant pressure and a uniform contact can be only ensured on the middle region (from 2 cm to 5 cm) in the sample. Individual samples were additionally divided into three segments of one centimeter each defining three regions from 2cm to 3cm, 3cm to 4cm and 4cm to 5cm (or vice versa) over the measuring ruler as it can be seen in Figure 3.5.

Altogether, 72 data points were collected for each of the three humidity conditions, resulting in 216 data points collected for part 2 of this experiment.

### 3.4. Testing Conditions

The experiments were performed in an isolated humidity chamber with temperature and humidity control. Since the aim of this set of experiments was to evaluate the effect of humidity on the peeling strength, the temperature was held constant at  $\sim 23^\circ\text{C}$ . Due to the size of the room, the temperature fluctuated slightly, but remained within  $\pm 3.5^\circ\text{C}$  of the desired condition. This temperature fluctuation does not affect the performance of the experiment, since

the idea was to mimic the environmental conditions experienced by biological adhesive systems. Those conditions tend to present slight variations throughout the day.

The sample preparation was performed at a temperature of  $\cong 23^{\circ}\text{C}$  and a constant relative humidity of  $\cong 35\%$ .

In terms of the humidity, a traceable hygrometer (Figure 3.6. (A)) was used for accurate control, as well as a dehumidifier (Figure 3.6. (B)) to avoid moisture excess, and humidifiers (Figure 3.6. (C)) to increase moisture when needed. The conditions desired were to be in one of the three established ranges: low ( $\leq 35\%$  *Relative Humidity*), medium ( $\cong 55\%$  *Relative Humidity*) and high ( $\geq 75\%$  *Relative Humidity*). These relative humidity conditions were allowed to have fluctuation within realistic environmental conditions.



Figure 3.6. The traceable hygrometer (A) allows for precise adjustments of the temperature and RH, the dehumidifier (B) lowers the RH, and the humidifiers (C) increase the RH as needed.

## CHAPTER IV

### RESULTS AND DISCUSSION

To investigate the effect of the environmental humidity on the peeling angle dependent peeling strength, the selection of Magic Scotch Tape 3M® as a suitable material, the dependence of the peeling strength on the peeling angle for an acrylic-based pressure sensitive adhesives will be discussed. In addition, the findings in this report will be compared to reports in literature for synthetic adhesives, as well as biological systems focusing on the peeling test angle measurements for gecko dry adhesive and glycoprotein driven adhesion in spider silk. Finally, how the adhesion properties vary as a function of environmental humidity changes will also be discussed.

#### 4.1. Material Selection

With the aim of using the most suitable material for these experiments, one centimeter strips of Polyisoprene NATSYN 2200 from Goodyear Chemical was used as the testing material in accordance with the literature [17]. This material was anticipated to be optimal for reproducing Kendall's experiments, which yielded the analysis described in section 2.1 of this document.

However, after using this material in several trials without consistent results, and due to the difficulties in terms of time demanding processing, it was decided to use instead Masking Tape 3M<sup>®</sup>, which was assumed to be a more reproducible system. In this case, the width of the tape was ¾". Initially, the experiments were performed at room temperature (~25°C) and room relative humidity, which can range between 23% and 50%.

The results yielded by Masking Tape 3M<sup>®</sup>, were not consistent due to challenges in obtaining a constant speed at a constant load, which is required to determine the dependence of peeling strength on the peeling angle in the second part of the experiment.

A new material, Magic Scotch Tape 3M<sup>®</sup> was chosen after discovering that it has been used in peeling test experiments performed previously with good reproducibility results. [11]

For the purpose of confirming that the new material was a better option than the Masking Tape 3M<sup>®</sup>, optical microscopy test was performed. The magnification used was 2X.

The interfacial contact between the Masking Tape 3M<sup>®</sup> and the glass substrate Figure 4.1. (A), and the Magic Scotch Tape 3M<sup>®</sup> and the glass substrate Figure 4.1. (B), was observed. Clearly, the first image displays a less uniform dispersion of the adhesive in contact with the glass after applying the same pressure, by rolling over a weight of approximately 1 kg.

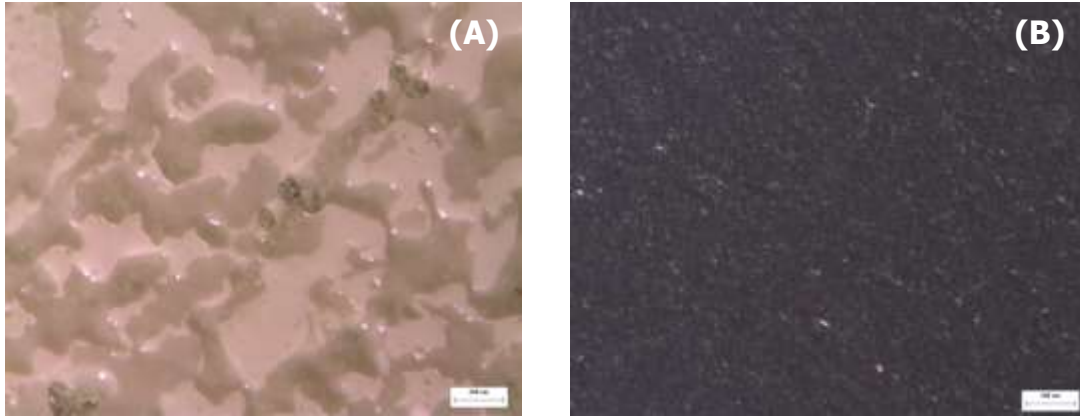


Figure 4.1. Optical Microscopy with 2X magnification, showing the contact homogeneity of (A) Masking Tape 3M® in contact with glass substrate and (B) Magic Scotch Tape 3M® in contact with glass substrate. Scale bar= 200  $\mu\text{m}$ .

Hamed and Hsieh showed that for an area that is totally bonded, the peeling force is higher in samples that contained small zones of non-contact in comparison with those that have larger non-contact zones [19]. From the microscopy images, we can see that the non-contact zones are larger in Masking Tape than in Magic Tape; this can be an explanation for the inconsistent results, considering that the Masking Tape 3M® is designed to be less adhesive to surfaces than other tapes because its applications demand that this tape be easily removed from the substrate. Thus, the glue coating is expected to be less uniform and the peeling force lower.

#### 4.2. Variation of Peel Strength with Crack Speed and Humidity Effect on Peeling Rate.

The results for this section were obtained in the same way as in Kendall's procedure. The speed was measured at different loads with a constant angle of 90°.

The speed was measured in a defined length of 10 mm and 9 data points were collected for each experimental configuration (see experimental section). The variation of 90° peel strength is equivalent to the adhesive energy  $R$ , and was measured with respect to the crack speed  $\dot{c}$ , as shown in Figure 2.2.

Samples were tested using loads of 30, 40, 50, 60, 70, 80 and 100 g. However, the speed values measured at loads greater than 70 g were not considered because these measurements could not be performed accurately using this specific set up. Evidence of the inaccuracy of the results obtained using loads greater than 70 g is shown in Table 1., where the dispersion of the data is demonstrate by the high standard deviations .

Table 4. 1 Speed measurement data at  $\pi/2$  ( $90^\circ$ )

Load (g)	35% RH			55% RH			75% RH		
	F/b (N/m)	Speed ( $\mu\text{m/s}$ )	Stand. Deviat.	F/b (N/m)	Speed ( $\mu\text{m/s}$ )	Stand. Deviat.	F/b (N/m)	Speed ( $\mu\text{m/s}$ )	Stand. Deviat.
30	46.299	45.609	3.005	46.299	262.602	23.286	46.299	1352.426	299.648
40	61.732	117.557	4.384	61.732	628.027	86.438	61.732	4094.202	209.309
50	77.165	212.834	18.572	77.165	1105.661	151.135	77.165	2407.471	506.190
60	92.598	277.794	26.546	92.598	1883.310	49.061	92.598	3165.025	309.772
70	108.031	2739.434	467.556	108.031	1542.383	27.160	108.031	4684.948	204.525
80	123.465	10088.975	3591.208	123.465	2065.268	396.219	123.465	10135.079	4397.732
100	154.331	16145.980	2718.653	154.331	-	-	154.331	6452.389	3082.298

Figure 4.2 shows the tendency of the crack speed to increase as the load increased. These results were compared with Kendall's findings, although the exact quantities were not expected to be the same since the material used was different in this experiment.

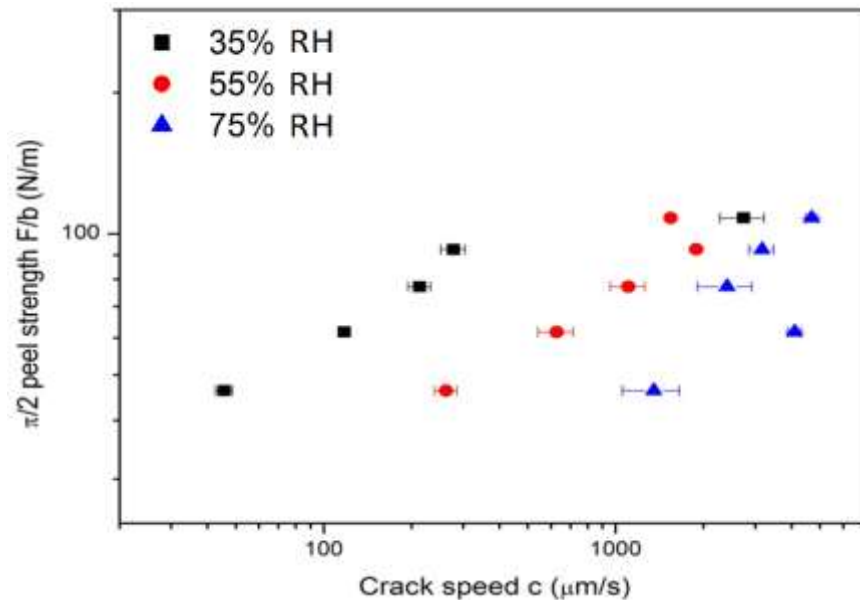


Figure 4.2. Variation of  $90^\circ$  peel strength with crack speed  $\dot{c}$ .



Previous studies have been performed to determine the correlation between peeling rate and peeling strength for a Polyisoprene adhered glass substrate [17]. Although the conditions used here are different, such as peeling angles of 80° and 135°, these previous experiments have shown the tendency of the peeling strength to increase as the angle increases, which is in agreement with the results yielded by Magic Scotch Tape 3M®.

On the contrary, variations in peeling strength with peeling rate measurements for hot melt pressure sensitive adhesives (HMPSA) produced interesting results for three samples that have the same formulation but different liquid/solid tackifying resin rates. These three samples were tested at 180° and 25°C, registering the highest peeling force for the sample with higher solid tackifier content and lower liquid content. [24]

The tendency of the peeling rate to increase as the peeling strength increased was the same for the three samples below 1200 mm/sec. After this point, the samples containing some amount of liquid resin continued to increase, whereas the sample containing only the solid resin displayed a significant drop in the peeling strength, possibly due to stick-slip fracture. This behavior was not observed in Magic Scotch Tape 3M®, where the composition remained constant for the duration of the experimental period.

The humidity effect on crack speed was also analyzed by examining the results presented in Figure 4.2. A displacement to the right, meaning an increase

in the crack speed range, was exhibited as the relative humidity increased from 35% to 75% at a constant temperature of 23°C.

Kendall presented the relationship between the adhesive energy ( $R$ ) and the peeling speed or crack speed ( $\dot{c}$ ) using the following function, which allows for the calculation of the adhesion energy with speed measured:

$$\frac{F}{b} = R(\dot{c}) \quad (5)$$

Considering this equation, the increase in the speed as the humidity increases can be interpreted as a decrease in the adhesion forces bonding the adhesive to the substrate.

Pressure sensitive adhesives are produced via emulsion polymerization of acrylic materials in water. This emulsion contains hydrophobic particles that are stabilized with surfactants. The exposure to humidity reduces the cohesive forces of the adhesive film, improving the ability of the material to flow and consequently increasing the peeling speed values [16].

Results regarding the humidity effect on the adhesion of polyimide films yielded similar results compared to results for the acrylic base adhesives, for the peeling strength as a function of the peeling rate at relative humidity values below 60% [28]. Measurements were performed at 23°C and RH: 30%, 40%, 51%, 60%, 70%, 82%. The tendency observed was a decrease in the peeling strength as the humidity increased, whereas the peeling strength and the peeling

rate have a linear relationship at a relative humidity up to 60%. These results support the results demonstrated here, and show that synthetic acrylic-based and imide-based adhesives possess the same peeling strength behavior as low (30%-35%) and medium (50%-60%) relative humidity is applied.

#### 4.3. Single Layer vs. Multi-layer Adhesive Systems

Magic Scotch Tape 3M® is a single coated tape that consists of at least four basic layers, as presented in Figure 4.3 [20]. The release coating is the treatment over the backing layer in charge of facilitating the unwinding of the material when applied, especially when high speed unwinding is required. The backing layer is also known as a carrier, made of Matte acetate of cellulose [21], and is a flexible thin film covered with the acrylic adhesive. This backing layer can be foil, paper, foam or any material according to the application of the tape. The primer is usually a liquid applied in the interface between the backing and the adhesive, and is used as bonding agent to increase the clinging ability between these two. The pressure sensitive adhesive layer corresponds to a mixture of acrylic water-based adhesives.

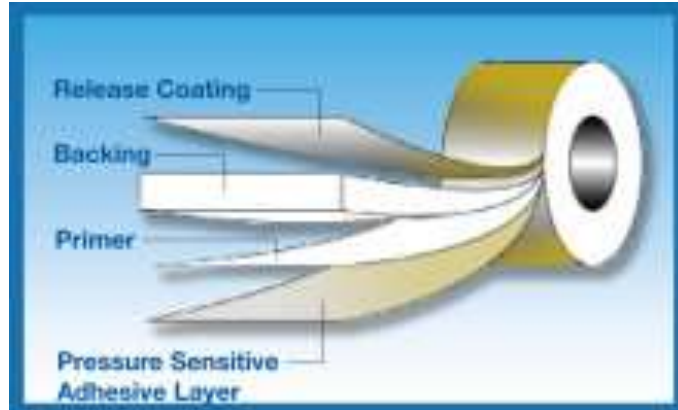


Figure 4.2. Schematic representation of a single coated pressure sensitive adhesive [20]

The system tested in this study was assumed to be inextensible, composed of a piece of Magic Scotch Tape 3M® attached to a rigid glass substrate previously cleaned as described in the experimental section.

The Rivlin equation considers the elastic term to be negligible, whereas in the Kendall equation the elastic term is highly relevant and must be taken into account for elastomers at low peeling angles (below  $30^\circ$ ); under these circumstances, the tape is considered to be an extensible elastic material [4]. The important impact of elasticity on peeling force at small peeling angles is presented in Figure 4.4, where the peeling force increased dramatically as detected on the results for angles of  $15^\circ$  and  $30^\circ$  at the 3 different humidity levels. Peeling force as a function of peeling angle was studied before using Magic Scotch Tape 3M® adhered to rigid glass substrate, and despite the use of a different experimental setup (including a translation stage and a load cell), the

results support the observations made using Kendall's device, particularly the tendency of the peeling force to decrease as the peeling angle increases [11].

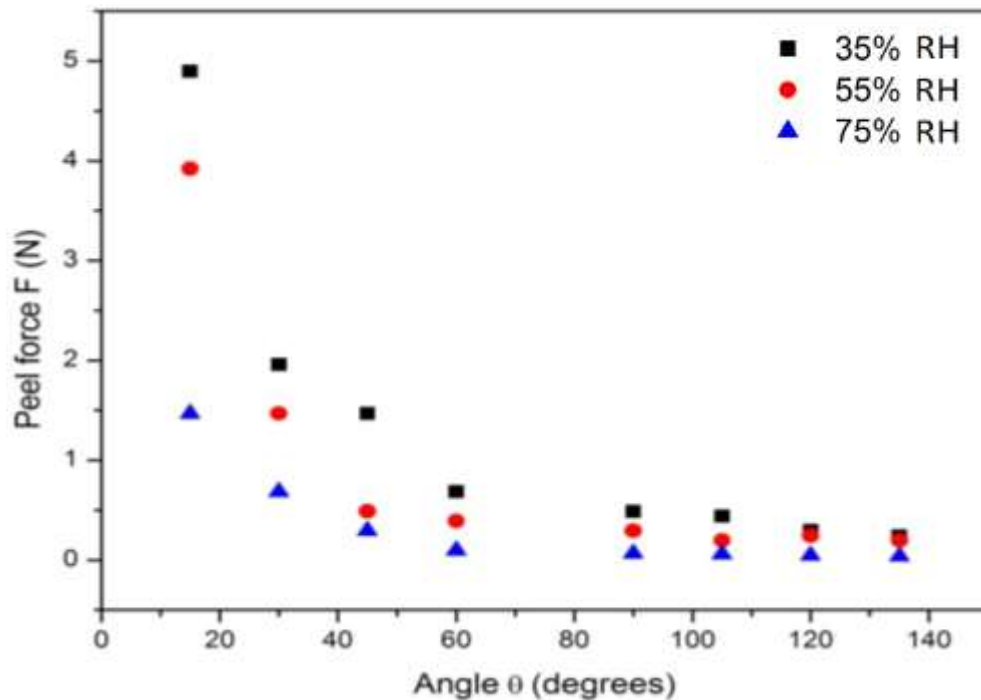


Figure 4.3. Relationship between the peel force and the peel angle.

The Elastic Modulus reported for Magic Scotch Tape 3M<sup>®</sup> is 1.65 GPa, and at this point we still ignore if the humidity effect is only over the adhesive or also over the other layers of the tape thus comparison of this tendency with results from previous research could be imprecise.

It is worth highlighting that both the Kendall and Rivlin models are designed to describe single layer thin elastic adhesive film, which in this case

corresponds only to the acrylic adhesive coating and not to the multilayer materials described previously in this section.

#### 4.4. Effect of Humidity on the Peeling Strength Dependent on the Peeling Angle

The effect of humidity was evaluated and the results were compared with two main two pre-existent models, Rivlin and Kendall. Both models were used to validate the experimental protocol to determine the dependence of the Peeling Strength on the Peeling Angle, as well as the effect of low, medium, and high humidity on the peeling strength as the angle changes. The fitting parameter selected is  $R$ .

In Figure 4.5, the fitting curves corresponding to Rivlin's Model for low, medium and high humidity ranges are presented. As mentioned in previous sections, this model does not consider the elastic term as part of the peeling process.

The Magic Scotch Tape 3M<sup>®</sup> was expected to follow Rivlin's model more closely, due to the high elastic modulus contributed from the rigid backing layer that provides characteristics of a non-elastic film, allowing the elastic term to be considered negligible. However, the results show that Kendall's Model represents this system much more accurately, as shown in Figure 4.6.

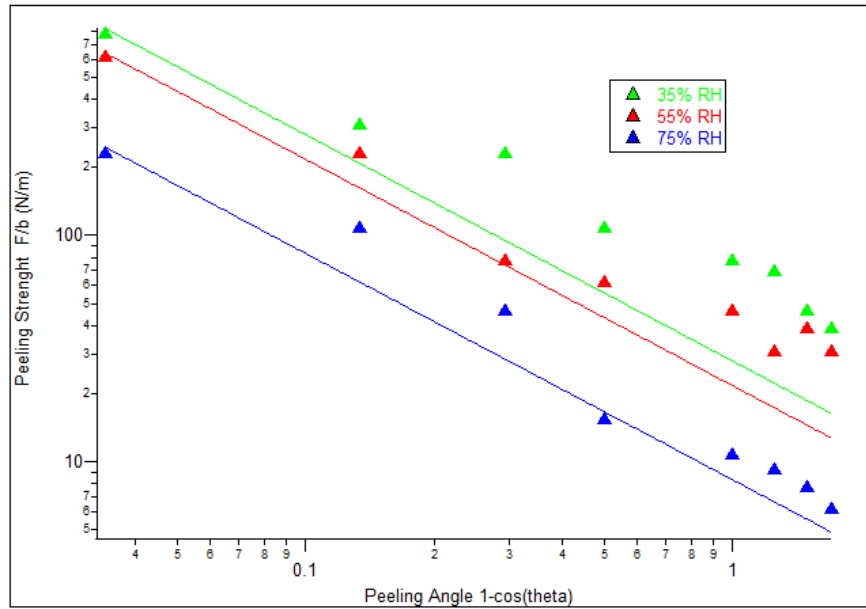


Figure 4.4. Rivlin Model for the peel strength dependence on peel angle at low (green), medium (red) and high (blue) relative humidity. Measurements taken at crack speed range between 200  $\mu\text{m/s}$  to 300  $\mu\text{m/s}$ .

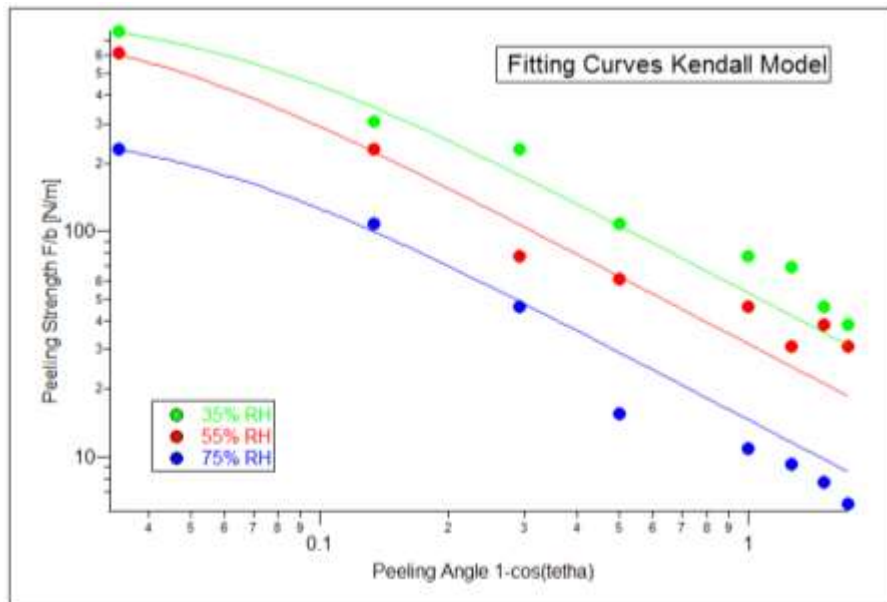


Figure 4.5. Kendall Model for the peel strength dependence on peel angle at low (green), medium (red) and high (blue) relative humidity. Measurements were taken at a crack speed range between 200  $\mu\text{m/s}$  to 300  $\mu\text{m/s}$ .

The approximation used for Rivlin's Model is a linear function:

$$\frac{F}{b} = \frac{R}{(1 - \cos\theta)} \quad (7)$$

Whereas Kendall's model uses a quadratic approximation:

$$\frac{F^2}{2Eb^2d} + \frac{F}{b}(1 - \cos\theta) = R \quad (8)$$

Where F corresponds to the applied force, which in turn is dependent on the load hanged as:  $F = m * g$ .  $R \left[ \frac{N}{m} \right]$ , is the adhesion force,  $b = 0.00635 \text{ m}$  is the width of the tape,  $\theta$  is the peeling angle,  $d = 6.25 \times 10^{-5} \text{ m}$  is the thickness of the tape [21], and  $E = 1,650,000,000 \frac{N}{m^2}$  is the elastic modulus reported for Magic Scotch Tape 3M®[11].

In order to simplify Kendall's equation, a new term B was introduced. This term combines the thickness and the elastic modulus as:

$$B = 2dE \quad (9)$$

IGOR Pro was used to analyze the experimental data and the results obtained from the fitting curves are presented in Table 4.2.



Table 4. 2. Results obtained from the fitting curves and calculated elastic modulus

		<b>35%</b>	<b>55%</b>	<b>75%</b>
<b>Rivlin</b>	$R \left[ \frac{N}{m} \right]$	$27.898 \pm 2.46$	$21.714 \pm 1.06$	$8.341 \pm 0.63$
<b>Kendall</b>	$R \left[ \frac{N}{m} \right]$	$53.394 \pm 4.99$	$31.663 \pm 1.23$	$14.61 \pm 1.06$
	$B \left[ \frac{N}{m} \right]$	$21,563 \pm 4.81e+003$	$33,956 \pm 2.97e+003$	$8,025.9 \pm 1.53e+003$
	E calculated $\left[ \frac{N}{m^2} \right]$	172,504,000	271,648,000	64,207,200

It has been shown that Kendall's Model better describes the behavior of the peeling phenomena.

The decreasing peeling strength as the peeling angle increases, displayed by the experimental data, concurs with the tendency of Kendall's theory. Thus the elastic term should definitely be considered for the analysis of this system.

Studies on peeling for the same material at different peeling angles have been performed using a different experimental design [11]. In this case, the inextensibility of tape was a common first assumption, allowing the elastic term to be neglected in the energy balance. The results obtained demonstrated the same correlation with Rivlin's and Kendall's fitting curves. However, the results related to be peeling force dependence on the angle are not conclusive, because

the considered data was collected at a minimum angle of  $30^\circ$  and above this angle the elastic contribution cannot be very well perceived.

The humidity effect on the peeling strength as the angle changes was also studied. This effect was noticed with the downward displacement of the data that means that the peeling force was decreased with increasing the humidity. As a result, the fitting curves also show that the peeling strength decreases as the humidity increases, in measurements performed maintaining a constant the peeling angle and targeting a constant crack speed.

The values calculated for the elastic modulus from the fitting curves at different ranges of humidity do not match the reported value for Magic Scotch Tape 3M<sup>®</sup>.

This can be attributed to a number of different causes. Since the material is a water-based acrylic adhesive, hygroscopic behavior can be expected as the surfactants and acrylic components plasticize when exposed to moisture [16]. The plasticization would have a direct effect not only in the interface between the adhesive and the substrate (penetration of water in the interface), but also in the bulk of the adhesive, changing its elastic properties.

Further measurements of the elastic modulus of the multi-layer tape in comparison with the elastic modulus of the single layer acrylic adhesive and the backing paper, are required to confirm if the elastic modulus values calculated

from experimental data at low, medium and high relative humidity, correspond to the elastic modulus of the single layer adhesive as we hypothesized.

Additionally, it is appropriate to consider that humidity can be also affecting the backing paper and the primer layer of the tape; measurements of water absorption of the tape and the backing paper separately are suggested to probe this statement.

Previous studies of the humidity effect on PMMA adhesives on glass substrate focused on the water concentration and water absorption [27]. Additionally, the results show a decrease in the adhesion strength of PMMA as the relative humidity increases. These results are in agreement with the results obtained for acrylic based adhesives, at least in the range of the measurements that were taken here.

Since studies in peeling have a major impact in the analysis of the biomechanics of bioadhesives, different approaches have been explored to understand the adhesion properties especially for gecko toe and spider silk.

Numerical-theoretical approaches have been presented to validate the assumptions related to the elastic modulus, length, roughness, peeling force and peeling angle, as well as their effect on the viscoelastic properties of a biomimetic film on a substrate [29]. Finite element method (FEM) has shown that there is an inversely proportional relationship between the peeling force and

the peeling angle, which is consistent with the experimental results shown above for an acrylic-based synthetic adhesive.

Other approximations to biological systems have been performed using synthetic bio-inspired materials, for instance "*Carbon nanotube-based synthetic gecko tapes*" [30]. Peeling measurements were done to calculate the detachment energy [31] of this synthetic system from Teflon, Acrylate, Glass and Mica substrates at different angles. The results presented only include 45° measurements, because the elastic term should only be considered at low angles, below or equal to 45° peeling angle [31]. The results they presented do not show the peeling strength dependence on the peeling angle, but rather the variation of the peeling behavior of the gecko-synthetic tape from different substrates. Other substrates were not considered in our work, but are suggested for further investigation in this field [30].

The peeling angle has been also studied on the spider attachment discs [22]. The results reported in this particular case were obtained using a set-up that includes a nano-force sensor controlling the peeling rate, and focuses on the fiber extension. Measurements were taken at a peeling test angle of 180° in order to remove the elastic modulus influence on the peeling force, which is based on previous studies that demonstrated how low angles tend to enhance the adhesion of the spider silk nano-fibers [23]; this is also consistent with our results.

On the other hand, the humidity effect was studied in an independent manner for geckos and spider silk as well [25]. When experiments aimed at determining the temperature effect on the gecko adhesion were performed, it was discovered that the humidity plays an important role in the clinging behavior [5]. The results were particularly relevant at low temperatures of 12°C, where the ability to cling proved to increase with the increase in humidity as the geckos were exposed to relative humidity values of 30, 55, 70, 80%. However, this relationship was not detected at temperatures around 32°C. Surprisingly, this behavior is the opposite of the one presented in the results obtained for other synthetic tapes [26].

Interesting phenomena was found when spider silk was subjected to humidity changes, such as cyclic responses to humidity, which can be compared with the contractions shown by the human muscles [6]. In addition, the effect of humidity changes in the volume and extensibility of spider silk has been studied [23]. Nevertheless, a closer connection to our work can be found in results of studies that measured peeling forces under humidity variations for two different kind of spider silk, gumfoot silk and viscid silk [23]. The humidity effect was practically irrelevant for gumfoot glue, which is presumably humidity resistant, showing constant adhesion and elasticity as the humidity was varied. In contrast, an increase the adhesion performance was detected as the humidity increased, particularly for the viscid silk. The humidity effect was more obvious at medium humidity, where not only the adhesion strength had a significant increment, but the silk also had higher extensibility.

## CHAPTER V

### SUMMARY AND CONCLUSIONS

In conclusion, biological adhesive systems (such as gecko feet structural adhesives and adhesive spider silk fibers) represent a fine choice in the quest to improve pressure sensitive adhesives, especially when they need to be used under medium - high humidity environmental conditions, where they have shown a great performance (increase in peeling strength) in contrast with the commercial acrylic based PSAs.

The experiment described in this paper seems to be a suitable procedure to test one of the main adhesive properties- peeling strength in acrylic pressure sensitive adhesives - and can be used as a standardized way to evaluate the behavior of adhesives that perform at different angles and under extreme environmental conditions. Nonetheless, some considerations over this procedure are necessary if we aim to use it for biological systems testing. For instance, uniform contact is required between the adhesive and the substrate in order to find consistent results. Thus, biological systems should display this regularity when they are in contact with the substrate.

Finally, the use of the peeling test device should be carefully considered, and additional improvements should be made to the experimental procedure in order to ensure reproducibility. Other factors that contribute to difficulties in data collection and reproducibility include perturbations and external factors, such as vibration and tilting.

## REFERENCES

1. Benedek, I. *Pressure-Sensitive Adhesives and Applications*, 2nd ed.; Marcel Dekker, Inc.: New York, NY; **2004**.
2. Pan, H. *Effect of Surface, Interface and Adhesion Principle (I)*. Zhanjie. **2003**, 24(2), 40-45
3. Gent, A. N.; Hamed, G. R. *Peel Mechanics of Adhesive Joints*. Polym. Eng. & Sci. **1977**, 17(7), 462-466.
4. Kendall, K. *Thin-film Peeling – The Elastic Term*. J. Phys. D: Appl. Phys. **1975**, 8, 1449-1452.
5. Niewiarowski, P. H., Lopez, S., Ge, L., Hagan, E., & Dhinojwala, A. *Sticky Gecko Feet: The Role of Temperature and Humidity*. PLoS ONE, **2008**, 3(5), 1–7.
6. Agnarsson, I., Dhinojwala, A., Sahni, V., & Blackledge, T. *Spider Silk as a Novel High Performance Biomimetic Muscle Driven by Humidity*. The Journal of Experimental Biology, **2009**, 212 (Pt 13), 1990–1994.
7. Edelman, J., *A Brief History of Tape*. Ambidextrous Magazine: Issue Five, **2006**. [Cited 2015 28.05]; Available from: [ambidextrousmag.org/issues/05/pdf/i5p45\\_46.pdf](http://ambidextrousmag.org/issues/05/pdf/i5p45_46.pdf)
8. Israelachvili, J.N. *Intermolecular and Surface Forces*, **2011**, Third Edition.
9. Bikerman, J.J. *Experiments on Peeling*. Journal of Appl. Pol. Sci. VOL. II, **1959**. ISSUE NO. 5. 216-224.
10. Bürgin, V., Daniels, A. U., Francioli, S., Schulenburg, J., & Wirz, D. *90° Peel off Tests of Tissue Engineered Osteochondral Constructs: A New Method to Determine the Osteochondral Integration*. International Journal of Tissue Engineering Volume **2014**, Article ID 343182, 6 pages.



11. Kovalchic, C., Ravichandran, G., Molinari, A. *Mechanics of Peeling for Extensible Elastic Adhesive Tapes*. 11th Pan-American Congress of Applied Mechanics. January 04-08, **2010**, Foz do Iguaçu, Brazil.
12. Pesika, N. S., Tian, Y. *Peel-Zone Model of Tape Peeling Based on the Gecko Adhesive System*. The Journal of Adhesion. **2007**, 83: 383 – 401.
13. Jin, K., Cremaldi, J. C., Erickson, J. S., Tian, Y., Israelachvili, J. N., & Pesika, N. S. *Biomimetic Bidirectional Switchable Adhesive Inspired by the Gecko*, Adv. Funct. Mater. **2014**, 24, 574-579.
14. Roenbeck, M. R., Wei, X., Beese, A. M., & Naraghi, M. *In Situ Scanning Electron Microscope Peeling To Quantify Surface Energy between Multiwalled Carbon*. ACS NANO. **2014** Vol. 8. No 1. 124-138
15. Brely, L., Bosia, F., Pugno, N. M., & Giuria, P. *Numerical Implementation of Multiple Peeling Theory and its Application to Spider Web Anchorages*. Interface Focus 5: 20100051. **2015**
16. Houtman, C., Severtson, S., Guo, J., Xu, H., & Gwin, L. *Properties of Water-based Acrylic Pressure Sensitive Adhesive Films in Aqueous Environments*. TAPPI 8th Research Forum on Recycling, **2007**. 1–6.
17. Wang, Y. *The Effect of Peeling Rate and Peeling Angle on the Peeling Strength*. The University of Akron, **2014**.
18. 5960 *Dual Column Testing Systems for Tensile, Compression, Flexure, Peel testing*. INSTRON USA. **2014**. [Cited 2014 22.11]; Available from: <http://www.instron.com/en-us/products/testing-systems/universal-testing-systems/electromechanical/5900/5960-dual-column?region=North%20America>
19. Hamed G.R. and Shieh C.H. *Relationship between the Cohesive Strength and the Tack of Elastomers*. J. Polymer Physics, **1983**. 21, 1415.
20. TESA TAPE, INC. *Understanding the Basics of Pressure-Sensitive Tapes*. **2015**. [Cited 2015 15.06]; Available from: [http://www.tesatape.com/featured/technology\\_journal/tape-101-understanding-the-basics-of-pressure-sensitive-tapes,8805648,1.html](http://www.tesatape.com/featured/technology_journal/tape-101-understanding-the-basics-of-pressure-sensitive-tapes,8805648,1.html)
21. Product Information 3M Stationery and Office Supplies Division. *Scotch™ No. MAGIC™ TAPE*. **2015** [Cited 2015 15.06]; Available from: [Pro link.browseproducts.net/WebCategoryImages/147/810.pdf](http://link.browseproducts.net/WebCategoryImages/147/810.pdf)

22. Jain, D., Sahni, V., & Dhinojwala, A. *Synthetic Adhesive Attachment Discs Inspired by Spider's Pyriform Silk Architecture*. Journal of Polymer Science, Part B: Polymer Physics, **2014**. 52(8), 553–560.
23. Sahni, V., Blackledge, T. a., & Dhinojwala, A. *Changes in the Adhesive Properties of Spider Aggregate Glue during the Evolution of Cobwebs*. Scientific Reports, **2011**. 1, 1–8.
24. Tsaur, A.T.; Tsaur, T. *Peel Adhesion as a Function of Peel Angle, Peel Rate, and Peel Temperature*. Pressure Sensitive Tape Council Files. **2011**.
25. Prowse, M. S., Wilkinson, M., Puthoff, J. B., Mayer, G., & Autumn, K. *Effects of humidity on the mechanical properties of gecko setae*. Acta Biomaterialia, **2011**. 7(2), 733–738.
26. Kovalchick, C., Molinari, A., & Ravichandran, G.. *Rate Dependent Adhesion Energy and Nonsteady Peeling of Inextensible Tapes*. Journal of Applied Mechanics, 81, **2014**.
27. Tan, K. T., Vogt, B. D., White, C. C., Steffens, K. L., Goldman, J., Satija, S. K., Hunston, D. L.. *On the Origins of Sudden Adhesion Loss at a Critical Relative Humidity : Examination of Bulk and Interfacial Contributions*. Langmuir. **2008**. 9189–9193.
28. Hu, D. C., & Chen, H. C. *Humidity Effect on Polyimide Film Adhesion*. Journal of Materials Science, **1992**. 27(19), 5262–5268.
29. Peng, Z. L., Chen, S. H., & Soh, a. K. *Peeling Behavior of a Bio-inspired Nano-film on a Substrate*. International Journal of Solids and Structures, **2010**. 47(14-15), 1952–1960.
30. Ge, L., Sethi, S., Ci, L., Ajayan, P. M., & Dhinojwala, A. *Carbon nanotube-based synthetic gecko tapes*. Proceedings of the National Academy of Sciences of the United States of America. **2007**. 104(26), 10792–10795.
31. Gent A.N., Kaang S.Y. Effect of Peel Angle upon Peel Force. The Journal of Adhesion. **1987**. 24:173–181.

## APPENDICES

## APPENDIX A

### PEELING STRENGTH DEPENDENT ON THE PEELING ANGLE DATA COLLECTED AT LOW RELATIVE HUMIDITY ( $\leq 35\%$ )

<b>T (°C)</b>	<b>HR (%)</b>	<b><math>\theta</math> (Degrees)</b>	<b><math>(1-\cos \theta)</math></b>	<b>Load (Kg)</b>	<b>F (N)</b>	<b>F/b (N/m)</b>	<b>Speed (<math>\mu\text{m/s}</math>)</b>	<b>St. Dev.</b>
21.7	33.7	15	0.034	0.500	4.900	771.654	217.688	92.566
23.5	36.6	30	0.134	0.200	1.960	308.661	305.920	95.884
23.1	32.8	45	0.293	0.150	1.470	231.496	268.936	101.818
26.6	28.9	60	0.500	0.070	0.686	108.031	255.227	78.824
21.6	35.4	90	1.000	0.050	0.490	77.165	229.738	87.808
22.2	33.3	105	1.259	0.045	0.441	69.449	248.455	182.290
24.8	32.3	120	1.500	0.030	0.294	46.299	281.140	150.852
24.0	34.9	135	1.707	0.025	0.245	38.583	240.243	55.193

## APPENDIX B

### PEELING STRENGTH DEPENDENT ON THE PEELING ANGLE DATA COLLECTED AT MEDIUM RELATIVE HUMIDITY ( $\cong 55\%$ )

<b>T (°C)</b>	<b>HR (%)</b>	<b><math>\theta</math> (Degrees)</b>	<b><math>(1-\cos\theta)</math></b>	<b>Load (Kg)</b>	<b>F (N)</b>	<b>F/b (N/m)</b>	<b>Speed (<math>\mu\text{m/s}</math>)</b>	<b>St. Dev.</b>
23.7	54.5	15	0.034	0.400	3.920	617.323	239.523	63.568
22.6	55.9	30	0.134	0.150	1.470	231.496	201.450	47.794
23.6	55.1	45	0.293	0.050	0.490	77.165	301.101	76.670
24.5	57.3	60	0.500	0.040	0.392	61.732	233.620	78.824
20.7	52.0	90	1.000	0.030	0.294	46.299	243.547	56.189
21.8	55.9	105	1.259	0.020	0.196	30.866	274.023	76.492
22.1	55.5	120	1.500	0.025	0.245	38.583	261.097	119.494
22.6	56.4	135	1.707	0.020	0.196	30.866	268.111	96.059

## APPENDIX C

### PEELING STRENGTH DEPENDENT ON THE PEELING ANGLE DATA COLLECTED AT HIGH RELATIVE HUMIDITY ( $\geq 75\%$ )

<b>T (°C)</b>	<b>HR (%)</b>	<b><math>\theta</math> (Degrees)</b>	<b><math>(1-\cos\theta)</math></b>	<b>Load (Kg)</b>	<b>F (N)</b>	<b>F/b (N/m)</b>	<b>Speed (<math>\mu\text{m/s}</math>)</b>	<b>St. Dev.</b>
23.9	82.9	15	0.034	0.150	1.470	231.496	204.739	224.500
23.8	79.0	30	0.134	0.070	0.686	108.031	243.138	117.940
22.9	80.3	45	0.293	0.030	0.294	46.299	212.067	92.150
25.1	84.0	60	0.500	0.010	0.098	15.433	237.838	63.571
25.5	84.1	90	1.000	0.007	0.069	10.803	273.399	75.640
23.3	82.2	105	1.259	0.006	0.059	9.260	333.288	126.687
24.4	84.2	120	1.500	0.005	0.049	7.717	295.800	103.628
23.3	82.2	135	1.707	0.004	0.039	6.173	270.335	75.860